This paper first appeared in the thirteenth print edition of the *Photovoltaics International* journal, published in August 2011.

Atomic layer deposition of Al_2O_3 for industrial local Al back-surface field (BSF) solar cells

Aude Rothschild, **Bart Vermang** & **Hans Goverde**, imec, Leuven, Belgium

ABSTRACT

Al_2O_3 deposition has received a lot of attention in the last few years for its attractive passivation properties of c-Si surfaces. Within the local Al back-surface field (BSF) cell concept, we considered several avenues of study: surface preparation, thermal stability, charge investigation and the 'blistering' phenomenon. The investigations converged on a passivation stack that includes a thin interfacial SiO_2-like layer and a thin Al_2O_3 layer (~10nm), which undergoes a high-temperature anneal (> 600°C). In order for a surface passivation with Al_2O_3 to be a cost-effective step for the PV industry, a high Al_2O_3 deposition rate is required. Compared to the different high-throughput tools that have recently emerged on the PV market, such as atomic layer deposition (ALD) and plasma-enhanced chemical vapour deposition (PECVD), our tool screening revealed quite similar results. The differences therefore seem to have an origin primarily in the tool specifications rather than in the achievable Al_2O_3 material properties.

Introduction

The atomic layer deposition (ALD) technique has its roots in the 1960s, but it was only in the mid 1990s that the semiconductor industry started to pay attention to this technique, to satisfy the demands of the ever-shrinking dimensions of CMOS devices. The reason for such interest comes from the fact that ALD offers excellent thickness and uniformity control at the nanometre level, on top of the fact that ALD layers can be deposited in a conformal way in structures of high aspect ratio, making ALD suitable for 3D structures as well.

For some years, ALD for photovoltaic applications, in particular ALD-Al_2O_3, has been gaining interest for new c-Si solar cell generations too [1–5]. As a major difference from most other dielectrics, such as Si_xN_y or SiO_2, where fixed positive charges are stored at the interface region, Al_2O_3 can lead to the presence of negative charges at the silicon surface. These negative charges induce a field effect, which repels the minority carriers at the interface and thereby

enhances the passivation level reached on *p*-type surfaces. However, in order to be applicable to industrial solar cell manufacturing and cost effective in solar applications, conventional ALD has to find a way to be compatible with high-throughput and high-yield requirements.

Given a fairly low deposition rate of about 1–5nm/min and the throughput requirement of solar cell manufacturers (currently about one 156 × 156mm^2 wafer/s), equipment vendors have tackled the challenge from two different directions: either by tweaking 'temporal' ALD into 'spatial' ALD or by adjusting the batch size ('batch' ALD). Two companies, Solaytec and Levitech, have built their tools (PDT and Levitrack) based on the first approach, which offers ALD deposition rate in the nm/s range. On the other hand, the companies ASM and Beneq have chosen the second approach, producing the batch ALD tools A412 and TFSNX300, respectively. A plasma ALD approach appears to be another possible option, but is not currently available for high-throughput applications.

Al_2O_3 deposition, however, is not restricted to the ALD approach: there are also other techniques available on the PV market, for example plasma-enhanced chemical vapour deposition (PECVD) (such as the SiNA system from Roth&Rau) and reactive sputtering.

Some potential applications of ALD-Al_2O_3 layers in future solar cells are the rear-side passivation of *p*-type c-Si substrates in PERL-type (passivated emitter, rear locally diffused) solar cells, and the front-side passivation of *p*-type emitters on *n*-type c-Si substrates, such as i^2-BC (industrial interdigitated back contact) solar cells [6]. ALD-Al_2O_3 could also serve as a tunnelling barrier layer for metal-insulator-semiconductor (MIS) contacts [7]. Each of these applications might eventually require a different passivation stack (different cleaning, annealing, additional layer, etc.) to satisfy the electrical and optical requirements.

This paper concentrates on the concept of a PERL-type local Al back-surface field (BSF) solar cell and the steps towards improving its rear-side passivation stack with Al_2O_3. Among the different process parameters that can improve the passivation level, two important aspects will be discussed in more detail: the surface preparation before the Al_2O_3 deposition [8] and the thermal stability of the layer, as in the 'contact firing' treatment in typical local Al BSF process flow [9]. In the next part of the paper, the focus will be on the charge characterization of the c-Si/SiO_2/Al_2O_3 passivation stack. This will be followed by addressing another important aspect that appears to be relevant when integrating Al_2O_3 into a local Al BSF process flow: the outgassing from Al_2O_3 layers that can cause blistered regions on the surface of rear-side passivation stacks (Al_2O_3/Si_xN_y) [10]. To conclude, we discuss the advances recently made in high-throughput Al_2O_3 tools and imec's position in that respect.

Surface preparation

The ALD process is very surface sensitive and therefore surface preparation prior to deposition of any passivation layer is a key parameter of the technique. This parameter will determine the physical properties (such as layer closure, density and roughness) and the electrical properties of the c-Si/dielectric interface (such as interface trap density D_{it} and fixed charges Q_f). As a consequence, the surface preparation before Al_2O_3 deposition will have an impact on the passivation level.

"The ALD process is very surface sensitive and therefore surface preparation prior to deposition of any passivation layer is a key parameter of the technique."

The ALD reaction mechanism and its various growth per cycle (GPC) modes have been extensively studied within the semiconductor industry for

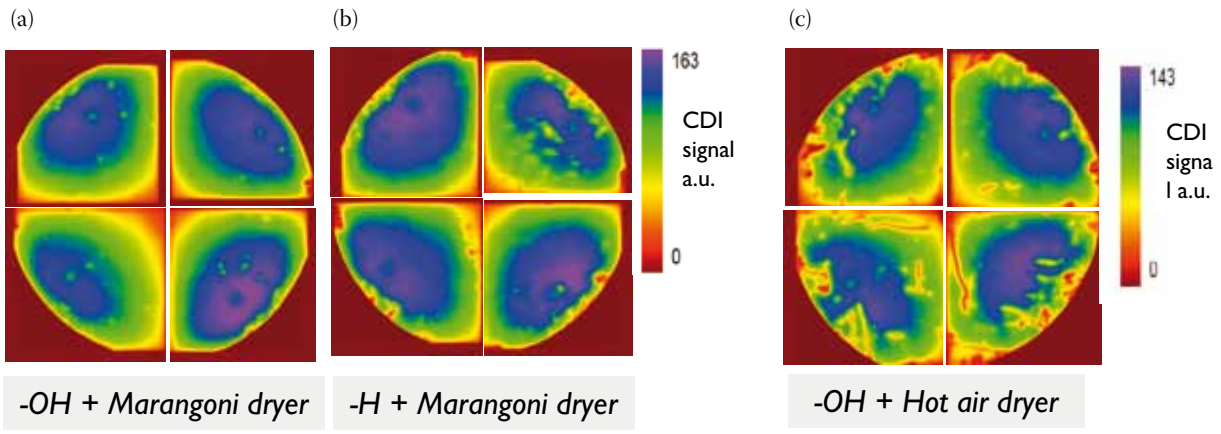

Figure 1. Comparison of passivation levels reached after annealing for different surface preparations before ALD-Al_2O_3 deposition: a) -OH terminated + Marangoni; b) -H terminated + Marangoni; c) -OH terminated + hot air dryer. Lifetime measurements were performed by carrier density imaging (CDI).

different high k layers (Al_2O_3, HfO_2, etc.) [11,12]. Besides many other parameters influencing the ALD growth of Al_2O_3 layers, such as precursor gas selection and deposition conditions, the surface preparation itself can strongly affect the initial interface growth mode type. It has often been reported that the *two-dimensional* growth mode (associated with a surface that is -OH terminated) is the preferred choice for its better transistor performance over the *island* growth mode (-H terminated) [13].

Drying of the surfaces after cleaning is just one of many influencing factors in the surface preparation prior to ALD deposition. In the semiconductor industry, a so-called Marangoni drying technique has become the standard drying process, resulting in wafers that are spotless and free of water marks, whereas the PV industry mostly uses a hot-air dryer approach.

Different surface treatments (-OH vs -H), in combination with two drying techniques (Marangoni vs hot air), have been studied for solar cell applications, taking into account the following criteria: a minimum level of defects, assessed by light scatterometry measurements; a wide within-wafer uniformity, evaluated by carrier density imaging (CDI); and a high minority-carrier lifetime level, measured by quasi-steady-state photoconductance (QSSPC).

As can be seen from Fig. 1, a hydrophilic clean (-OH) that is dried using the Marangoni technique leads to an improved surface passivation level and uniformity, as compared to the one dried by the hot air method. The surface preparation was performed using the following cleaning sequences: sulphuric peroxide mixture (SPM = H_2SO_4/H_2O_2) + HF/HCl + ammonium peroxide mixture (APM = $NH_4OH/H_2O_2/H_2O$), for the -OH terminated surface; and SPM + HF/HCl, for the -H terminated surface [8]. The 8" wafers were cut into four pieces for measurement

Figure 2. Interfacial SiO_2 regrowth is observed on a hydrophobic surface after annealing c-Si/3nm Al_2O_3 by FGA@350°C.

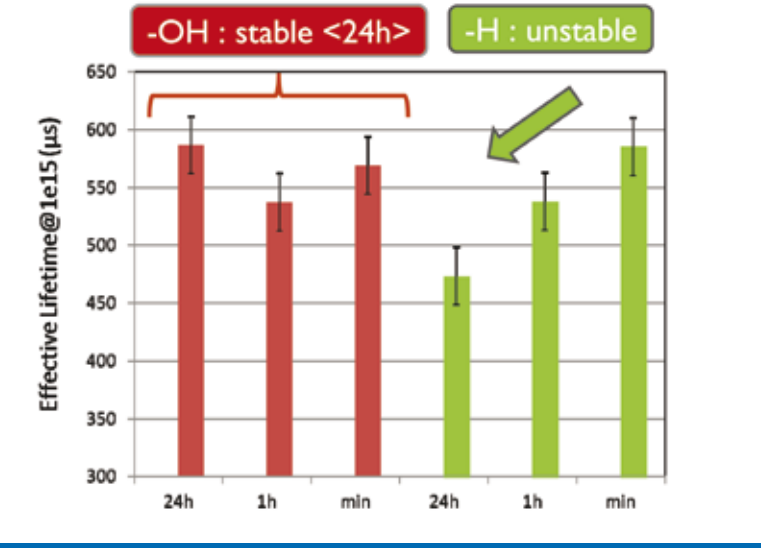

Figure 3. Stability of the passivation level over time for two types of clean: hydrophilic (-OH) vs hydrophobic (-H).

purposes, each piece receiving the same treatment. Surprisingly, the hydrophobic starting surface (-H) with Marangoni drying leads to a passivation level and uniformity similar to the hydrophilic clean. A physical analysis of the c-Si/Al_2O_3 interface indicates the growth of an SiO_2-like layer during the forming gas annealing (FGA) at 350°C (a low-temperature anneal in forming gas atmosphere). This growth reflects the H_2O release from the Al_2O_3 film during the annealing process, leading to an oxidation of the interface (Fig. 2). This is most likely the reason that similar passivation levels are reached after annealing for both hydrophilic and hydrophobic cleans, since both types will include an SiO_2-like interface.

However, a hydrophobic surface is more sensitive to moisture and hydrocarbons and its hydrophobicity is therefore time critical. Consequently, a hydrophilic clean is preferred for its stability over time: a hydrophilic state can be guaranteed for 24 hours, whereas a hydrophobic state will degrade within a few hours, affecting its passivation level (Fig. 3). This stability is of practical interest since it avoids the need to perform the clean/Al_2O_3 deposition steps in a short timeframe.

Thermal stability

There are reports in the literature regarding surface passivation studies (based on lifetime measurements) that are typically carried out on high-quality *p*- or *n*-type float-zone (FZ) material [14] with a high bulk lifetime in order to be sensitive to the contribution from the surface rather than from the bulk. However, one needs to make sure that the trends observed for FZ material remain valid for solar-grade Czochralski (CZ) material as well, especially regarding the thermal stability of Al_2O_3 above 800°C, which corresponds to the thermal budget of the firing step once integrated into a local Al BSF cell concept.

In that context, a study of CZ material has been undertaken, in which different Al_2O_3 thicknesses and thermal budgets were considered. Solar-grade *p*-type CZ material (2Ωcm) received saw damage removal (SDR) and polishing steps (160µm-thick final thickness) prior to passivation with ALD-Al_2O_3. The Al_2O_3 thickness deposited was in the range 5–30nm. The thermal budgets applied were either a low-temperature anneal (FGA@350°C) or a high-temperature anneal around 800°C (firing temperature) in order to determine the thermal budget limitations in low- and high-temperature regimes.

As can be seen in Fig. 4, for all Al_2O_3 thicknesses in a 5–30nm range, the passivation level is increased after FGA@350°C and is maintained for a firing thermal budget [9]. In terms of thermal stability, this CZ behaviour is therefore different from the one that is usually observed for FZ material. This difference illustrates the strong impact of the starting substrate in assessing the passivation level reached with Al_2O_3 and underlines the need for studying both substrates in parallel.

> "Besides thermal stability, the stability of Al_2O_3 over time is another important aspect to consider: the high passivation level reached with Al_2O_3 once annealing is performed has to be maintained."

The results shown in Fig. 4 also emphasize that the Al_2O_3 thickness required to achieve a high enough passivation level does not need to be excessive: approximately 10nm of Al_2O_3 is sufficient to reach a high passivation level, even after a high thermal budget. The minimum Al_2O_3 thickness is an important element for the high-throughput requirement that will be discussed later. Besides thermal stability, the stability of Al_2O_3 over time is another important aspect to consider: the high passivation level reached with Al_2O_3 once annealing is performed has to be maintained. This point is currently under investigation [15].

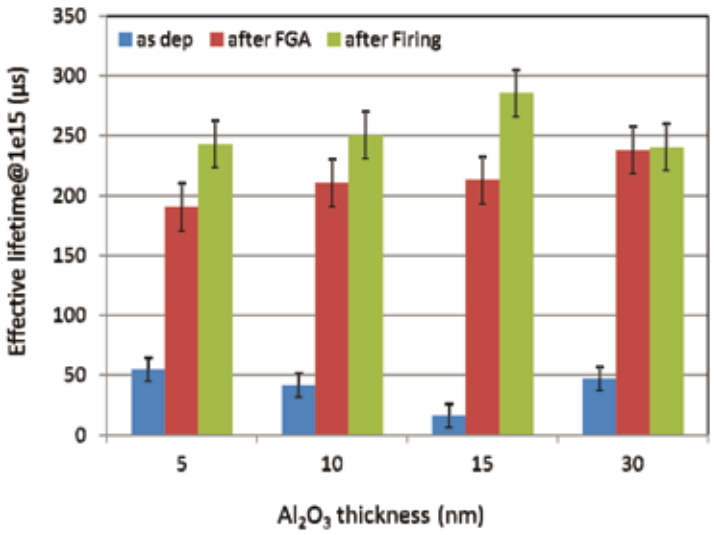

Figure 4. Thermal stability of different Al_2O_3 thicknesses on *p*-type CZ (2Ωcm), with SDR and polishing prior to passivation.

Charge characterization

Whereas other dielectrics such as SiO_2 and Si_xN_y introduce fixed positive charge Q_f, Al_2O_3 induces a build-up of negative fixed charge within the dielectric passivation stack [2]. This negative fixed charge, which induces a *field-effect* passivation, is considered to be one component that controls the low surface recombination velocity reached with Al_2O_3.

The second component is the *chemical* passivation, which is related to the interface trap density D_{it}. Benick et al. [16] reported that the weight of these two components is not the same, however, and that a low D_{it} is a prerequisite in order to benefit from the strong field-effect component.

Two approaches have been developed to investigate the electrical parameters and process parameters that control the passivation quality. The first (so-called *double-thickness series*) approach offers, through a statistical capacitance–voltage (CV) analysis, information related to charge polarity and charge quantity, as well as a decoupling of the location of the charge within the passivation stack c-Si/SiO_2/Al_2O_3 [17]. Fig. 5 shows a schematic of the model used for charge extraction at the different interfaces. The principle of the technique relies on the evolution of the flat-band voltage V_{fb} as a function of the equivalent oxide thickness EOT, according to Equation 1, where ϕ_{ms} is the work function difference between the metal and the semiconductor material, and $T_{Al_2O_3}$ corresponds to the EOT contribution of the Al_2O_3 layer to the total EOT. To be able to determine the different charge densities, independent variation of the SiO_2 thickness and Al_2O_3 thickness is required. From a straight-line fit of the V_{fb}–EOT plot of the SiO_2 thickness series, the slope allows extraction of the charge density at the interface Si/SiO_2 (Q_{Si/SiO_2}). Charge densities at the SiO_2/Al_2O_3 interface (Q_{SiO_2/Al_2O_3}) and in the bulk of the Al_2O_3 ($\rho_{Al_2O_3}$) can be estimated from the fit of the V_{fb}–EOT plot of the Al_2O_3 thickness series.

The experiment was performed using 8" 700µm-thick *p*-type CZ wafers. A slant-etched SiO_2 approach was followed, which has the advantage of increasing accuracy, avoiding wafer-to-wafer non-uniformity and enabling a large number of data points to be generated from each wafer. The SiO_2 slant-etch, performed by a controlled immersion speed at HF, was in the range 1–6nm and the Al_2O_3 thickness was in the range 2–30nm. FGA@350°C was then performed as the last processing step, to

$$V_{fb} = EOT\left[-\frac{Q_{Si/SiO_2}}{\varepsilon\,\varepsilon_{ox}}\right] + \left\{\varphi_{ms} - \frac{\rho_{Al_2O_3}\cdot T_{Al_2O_3}^{\,2}}{2\,\varepsilon\,\varepsilon_{ox}} - \frac{Q_{SiO_2/Al_2O_3}\cdot T_{Al_2O_3}}{\varepsilon\,\varepsilon_{ox}}\right\}$$

Equation 1.

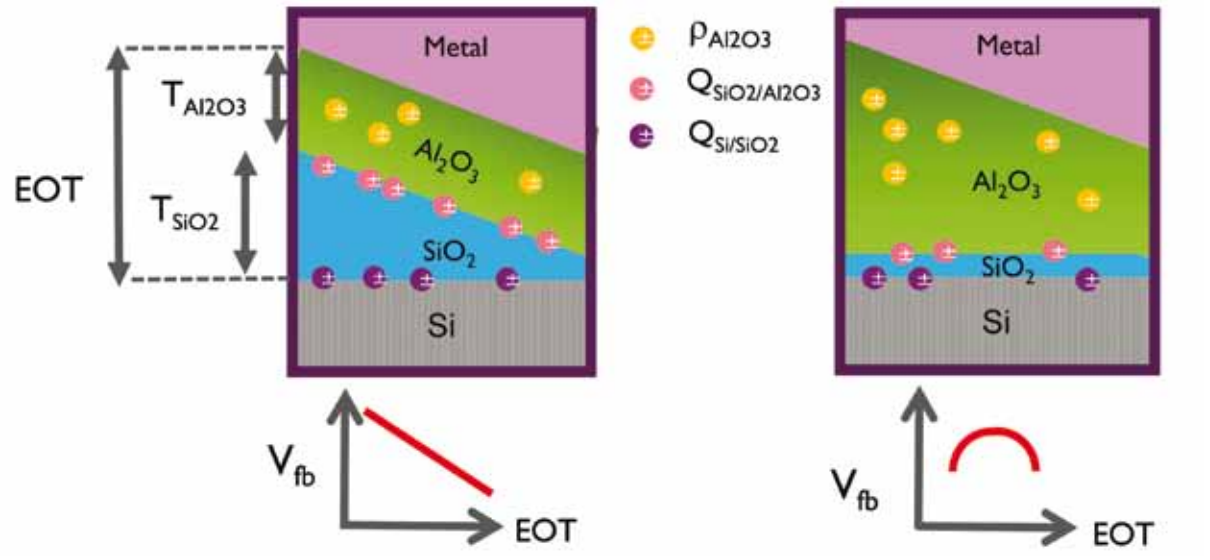

Figure 5. Charge extraction model – double-thickness series approach for determination of fixed charge within the passivation stack (Si/SiO_2/Al_2O_3): (a) varying only SiO_2 thickness enables Q_{Si/SiO_2} extraction; (b) varying only high-k thickness enables Q_{SiO_2/Al_2O_3} and $\rho_{Al_2O_3}$ extraction.

$Q_{Si/SiO2}$(cm^{-2})	$Q_{SiO2/Al2O3}$(cm^{-2})	ρ_{Al2O3}(cm^{-3})
2E+11	–4E+11	–1E+19

Table 1. Estimation of charge density and distribution within the c-Si/SiO_2/Al_2O_3 stack.

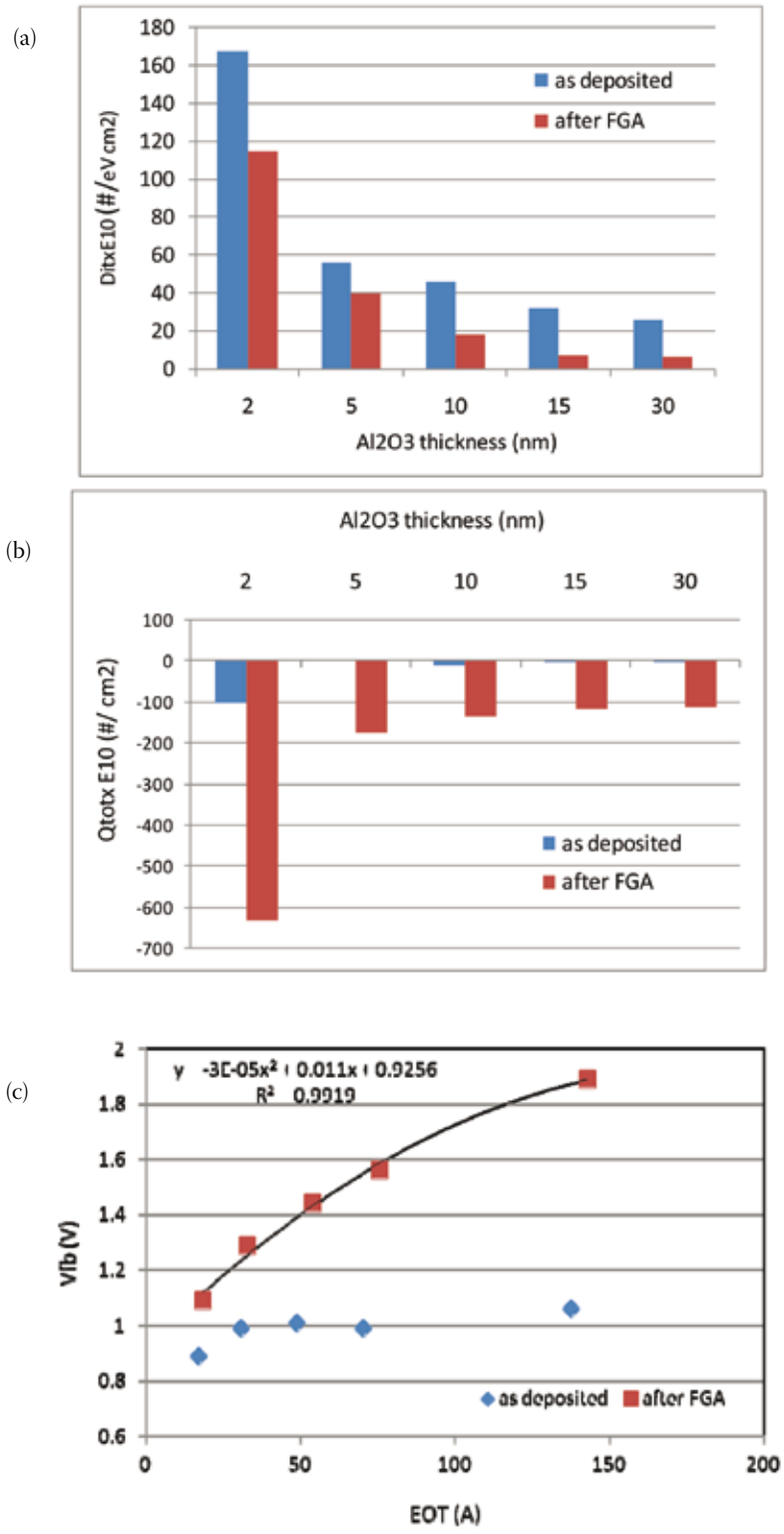

Figure 6. (a) Interfacial trap density D_{it} and (b) total amount of charge Q_{tot} extracted from V–Q measurements for Al_2O_3 as deposited and after FGA@350°C; (c) flat-band voltage versus equivalent oxide thickness EOT for Al_2O_3 as deposited and after FGA@350°C. The annealed samples exhibit a positive slope, indicating the presence of a global negative charge build-up within the c-Si/SiO_2/Al_2O_3 stack.

mimic the annealing performed within the thermal stability evaluation that was discussed earlier.

The results indicate positive fixed charge at the interface Si/SiO_2 (Q_{Si/SiO_2}>0), negative fixed charge at the interface SiO_2/Al_2O_3 (Q_{SiO_2/Al_2O_3}<0) and a non-negligible charge density in the Al_2O_3 bulk. Charge density at the Si/SiO_2 interface (Q_{Si/SiO_2}) is of the order of $+7\times10^{10}$cm^{-2}, but once the Al_2O_3 layer is deposited the amount of charge at this interface increases. The orders of magnitude of the different resulting charge densities are given in Table 1.

The negative fixed charge build-up by the deposition of Al_2O_3 is therefore rather complex. At the interface, the charge polarity and quantity reflect the signature of an SiO_2-like interface. The low D_{it}, as can be measured by CV or deep-level transient spectroscopy (DLTS) [18], is an electrical confirmation of the physical presence of an SiO_2-like layer.

The second methodology that was investigated was the *corona-charging technique*, which allows the consolidation of spatially resolved information on charge and carrier lifetime, in a fast learning cycle [19]. As can be observed from Figs. 6(a) and 6(b), D_{it} and the total amount of charge Q_{tot} depend on the Al_2O_3 thickness. Increasing the Al_2O_3 layer from 2 to 30nm leads to a reduction in D_{it}. This reduction is larger than the effect of the FGA itself, which is mostly visible for the very thin 2nm layer. Q_{tot}, which is a sum of different charge contributions, indicates a rather low amount of charge for the Al_2O_3 as-deposited samples. Once an FGA@350°C has been performed, the charge polarity becomes strongly negative, whatever the thickness of Al_2O_3 deposited.

This is clearly reflected by the flat-band voltage evolution vs EOT, which shows a positive slope, indicating a global negative-charge build-up in the c-Si/SiO_2/Al_2O_3 stack (Fig. 6(c)). The Al_2O_3 layer does not need to be excessively thin to minimize D_{it}, and at the same time the quasi-linear V_{fb}–EOT relationship when varying Al_2O_3 thickness indicates that fixed charges are located mostly at the interface. Increasing the Al_2O_3 thickness does not seem to play a major role.

The two approaches reveal the following information. First, the low D_{it} has the same signature as an SiO_2-like interface, indicating the key role of this interfacial layer in the passivation mechanism. Second, the global negative-charge density is in fact decoupled into two components: positive at the interface Si/SiO_2 and negative at the interface SiO_2/Al_2O_3. Third, a thin Al_2O_3 (5–10nm) provides the low D_{it} and amount of negative fixed charge required to passivate the surface, and there is no need to deposit a thicker Al_2O_3 layer.

'Blistering'

The integration of Al_2O_3 into solar cells has recently uncovered potential issues with the appearance of 'blisters' [20]. This phenomenon is a concern, since a local delamination of the Al_2O_3 layer, and therefore a reduction of the overall passivated area, decreases the cell performance. Investigation of outgassing behaviour and formation of blisters has consequently been conducted in more detail, and strategies to minimize their negative impact have been developed [10].

Annealing a sufficiently thick ALD Al_2O_3 layer and capping it with PECVD-Si_xN_y can lead to blister formation. A top-view scanning electron microscopy (SEM) picture of typical blistered Al_2O_3 layers can be seen in Fig. 7(a). The blisters can fully open when a high thermal budget is applied (during the firing step), thereby creating random local metal-semiconductor contacts. In order to investigate at which process step the blisters originate, thermal treatments were applied in the range 350–900°C. Atmospheric pressure ionization mass spectrometry (APIMS) was performed to detect any gas desorption within this temperature range. The thermal desorption spectroscopy (TDS) profiles indicate mainly the release of H_2O (m/e = 18 (H_2O^+)) and H_2 (m/e = 29 (N_2H^+)) around 400°C. The blistering phenomenon starts exactly when this gas desorption is first observed. One important parameter, which plays a role in whether or not blisters are present, is the Al_2O_3 thickness. As can be seen in Fig. 7(b), for a thin Al_2O_3 layer (≤ 10nm) there are no blisters, while for a thick layer (30nm) the blisters can be as large as a few microns. This illustrates the fact that the Al_2O_3 layer acts as a gas barrier and that the thicker the Al_2O_3 layer, the more pronounced the blister formation.

The blistering phenomenon is also intensified if the Al_2O_3 is capped with Si_xN_y, because the stack creates an even more effective gas barrier. In order to avoid blistering, a sufficiently thin Al_2O_3 layer is necessary and an outgassing step prior to the Si_xN_y capping and co-firing should be performed. The outgassing temperature should be chosen as a function of the Al_2O_3 thickness and of the firing temperature to be applied in the processing sequence. As shown in Fig. 8, an outgassing temperature above 600°C is adequate to avoid blistering for 5nm-thin Al_2O_3 layers in the passivation stack, whereas a temperature of 400°C is not. PERL-type solar cells with local Al BSF rear contacts having an Al_2O_3/Si_xN_y rear-side passivation stack were made using an outgassing step with temperatures up to 700°C. For these cells, the reduction in blistering, and hence improvement in rear surface passivation, is clearly reflected in the open-circuit voltage gain (V_{oc}) as a function of outgassing temperature (Fig. 9). Furthermore, after outgassing at 600 or 700°C, the Al_2O_3-passivated local Al BSF cells are clearly better passivated at the rear, compared to the SiO_2/Si_xN_y-passivated reference cells.

High throughput

So far, research on Al_2O_3 for passivation of solar cells has been carried out mostly on lab-scale reactors (Savannah from Cambridge Nanotech Inc. or FlexAL from Oxford Instruments). Although there is no doubt that the passivation results obtained with Al_2O_3 have potential for PV application, its implementation on an industrial scale is solely dependent on the throughput of the deposition technique and the costs associated with it. To reach such objectives, a technological breakthrough in the ALD deposition technique has been necessary. Equipment vendors have tackled the challenge from two different perspectives: either by extending the batch size concept further (e.g. ASM and Beneq with batch ALD) or by completely redesigning the concept itself (e.g. Levitech and Solaytec with their respective spatial ALD concepts). The approaches currently taken are:

1. **Spatial ALD:** the different precursor gases trimethylaluminium (TMA) and H_2O are spatially separated, and the wafers pass sequentially through the different deposition zones, which are appropriately surrounded by inert gas bearings to prevent the precursor gas flows from mixing.

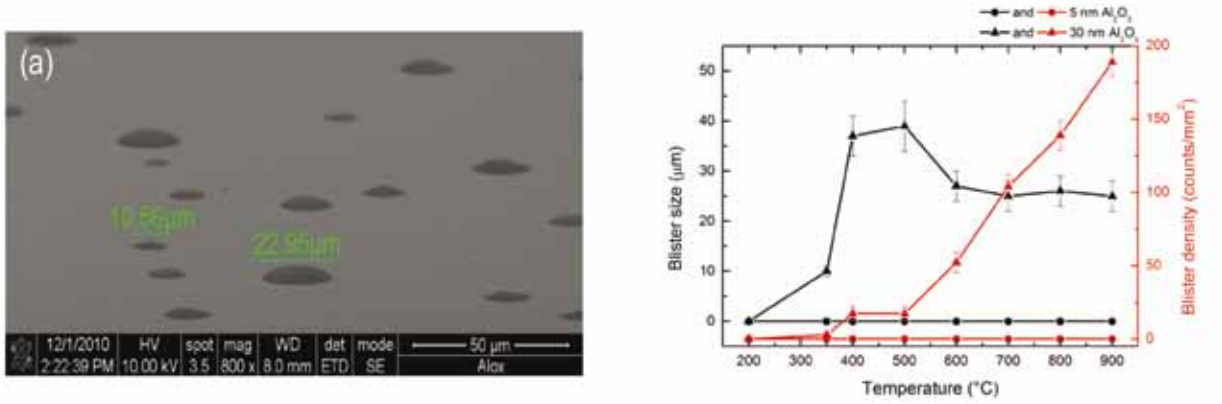

Figure 7. (a) Top-view SEM of a thick Al_2O_3 layer showing blister formation; (b) blister density and size as a function of annealing temperature (350–900°C) for both a thin and a thick Al_2O_3 layer.

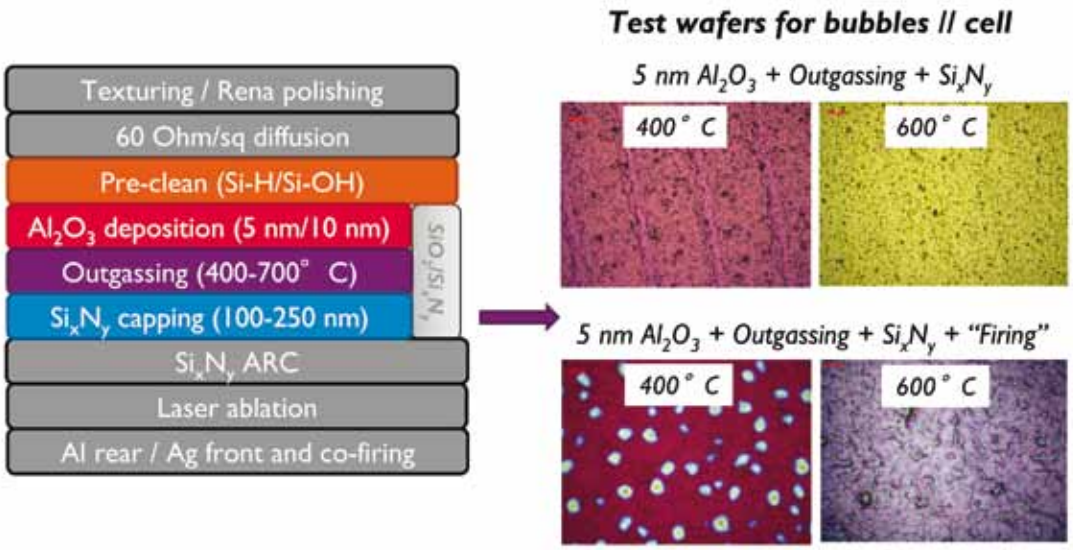

Figure 8. Blistering reduction with outgassing prior to Si_xN_y capping.

2. **Batch ALD:** this concept is based on conventional temporal ALD, where the deposition reaction is divided into two time-sequenced reactions – alternating TMA pulse and H_2O pulse, each one being separated by purge steps.

Imec has carried out a screening of the different high-throughput options, which include spatial ALD, batch ALD and PECVD. When comparing the deposition techniques side by side, the study did not uncover any major differences in terms of lifetime results, which tends to confirm previous data reported by Schmidt et al. [21]. In our opinion, the difference mostly comes from the process and hardware specifications (wafer size, wafer thickness, parasitic deposition, etc.) that the tools are able to achieve, rather than differences in Al_2O_3 material properties. Every tool on the market offering fast throughput Al_2O_3 claims to achieve the required throughput (> 3000 wafers/hour), under assumptions made for a 10nm Al_2O_3 deposition production process. What makes a difference is therefore linked to the tool design itself. The tool design and its impact on the process window, consumption of consumables (cost of TMA precursor gas is essential), yield and maintenance costs [22] appear to be the final criteria to consider.

Conclusions

Al_2O_3 appears to be a suitable candidate for passivation of *p*-type surfaces in a number of advanced solar cell concepts. In the case of PERL-type solar cells with local Al BSF rear contacts and a passivation stack on the rear side, a hydrophilic surface followed by the deposition of a thin Al_2O_3 layer and an outgassing step prior to completing the passivation stack seems to be the most suitable approach for achieving advantageous solar cell results, compared to a reference process with an SiO_x/Si_xN_y passivation stack that has been developed by imec in recent years [1]. High lifetime, no blistering and improved V_{oc} have been achieved using this approach, whereby Al_2O_3 is integrated into the passivation stack and processing sequence. Based on lifetime studies, no major differences were found when screening different high-throughput Al_2O_3 deposition tools. The tool selection seems to be more driven, therefore, by the process and hardware specifications than the Al_2O_3 material properties.

With respect to the future of ALD in PV manufacturing, Al_2O_3 can very likely be considered as a case study. If adequate efficiency improvement and cost of ownership numbers can be demonstrated, this could be the start of many other ALD applications within solar cell manufacturing, such as new materials (dielectrics, metals, etc.) and new applications for current and advanced technologies (antireflection coating, isolation, diffusion barrier, contacting layer, etc.). What makes ALD so special is only partially used today: *thickness control* is the major requirement in current cell technologies but the *conformality* aspect has not yet been explored very much (e.g. deposition on plasmonic structures

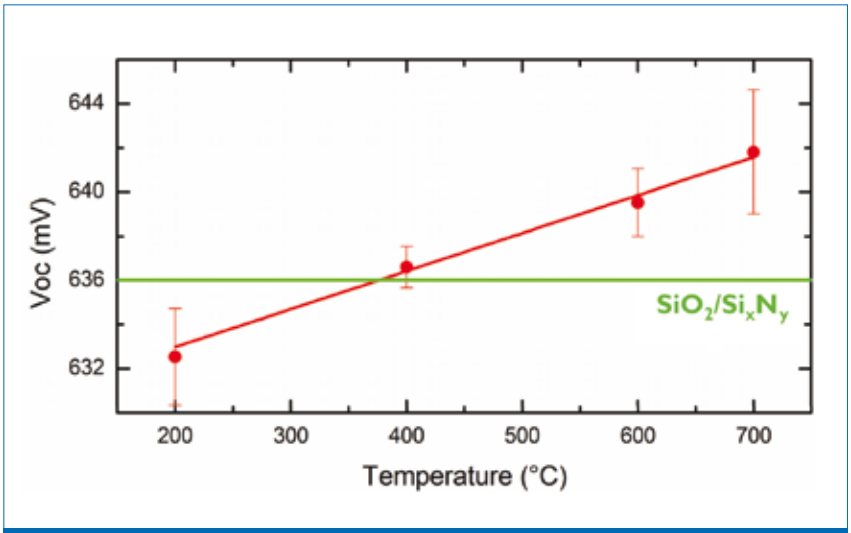

Figure 9. Increase in open-circuit voltage (V_{oc}) as a function of outgassing temperature. Higher values than the reference SiO_2/Si_xN_y passivation stack are reached.

and deposition on Si nanowires for Si multijunction solar cells). For advanced cell concepts, where high aspect ratio structures enter the equation, there is a good chance that ALD will make a difference compared to other deposition techniques. ALD has potentially a bright future, therefore, within solar cell manufacturing.

References

[1] Agostinelli, G. et al. 2006, "Very low surface recombination velocities on *p*-type silicon wafers passivated with a dielectric with fixed negative charge", *Solar Energy Mat. & Solar Cells*, Vol. 90, p. 3438.

[2] Hoex, B. et al. 2007, "Excellent passivation of highly doped p-type Si surfaces by the negative-charge-dielectric Al_2O_3", *Appl. Phys. Lett., Vol.* 91, p. 112107.

[3] Hoex, B. et al. 2008, "On the c-Si surface passivation mechanism by the negative chargedielectric Al_2O_3", *J. Appl. Phys.*, Vol. 104, p. 113703.

[4] Saint-Cast, P. et al. 2009, "Very low surface recombination velocity on *p*-type c-Si by high-rate plasma-deposited aluminum oxide", *Appl. Phys. Lett.*, Vol. 95, p. 151502.

[5] Dingemans, G. et al. 2010, "Silicon surface passivation by ultrathin Al_2O_3 films synthesized by thermal and plasma atomic layer deposition", *Phys. Stat. Sol. RRL*, Vol. 4, No. 1, p. 10.

[6] Reichel, C. et al. 2010, "Decoupling charge carrier collection and metallization geometry of back-contacted back-junction silicon solar cells by using insulating thin films", *Proc. 35th IEEE PVSC*, Honolulu, Hawaii, USA, p. 1034.

[7] Hezel, R. et al. 1997, "Recent progress in MIS solar cells", *Prog. Photovolt.*, Vol. 5, p. 109.

[8] Vermang, B. et al. 2010, "Surface passivation for Si solar cells: a combination of advanced surface cleaning and thermal atomic layer deposition of Al_2O_3", *Proc. 25th EU PVSEC*, Valencia, Spain, p. 1118.

[9] Rothschild, A. et al. 2011, "ALD-Al_2O_3 passivation for solar cells: firing stability", *Proc. 26th EU PVSEC*, Hamburg, Germany [in press].

[10] Vermang, B. et al. 2011, "On the blistering of atomic layer deposited Al_2O_3 as Si surface passivation", *Proc. 37th IEEE PVSC*, Seattle, Washington, USA [in press].

[11] Puurunen, R.L. 2005, "Surface chemistry of atomic layer deposition: A case study for the trimethylaluminum/water process", *J. Appl. Phys.*, Vol. 97, p. 121301.

[12] Puurunen, R.L. 2003, "Growth per cycle in atomic layer deposition: a theoretical model", *Chem. Vap. Deposition*, Vol. 9, p. 249.

[13] Green, M.L. et al. 2006, "Nucleation of atomic-layer-deposited HfO_2 films, and evolution of their microstructure, studied by grazing incidence small angle x-ray scattering using sychrotron radiation", *Appl. Phys. Lett.*, Vol. 88, p. 032907.

[14] Dingemans, G. et al. 2010, "Firing stability of atomic layer deposited Al_2O_3 for c-Si surface passivation", *Proc. 35th IEEE PVSC*, Honolulu, Hawaii, USA, p. 705.

[15] Penaud, J. et al. 2011, "Impact of ageing on AlO_x layer passivation properties for advanced cell architectures", *Proc. 37th IEEE PVSC*, Seattle, Washington, USA [in press].

[16] Benick, J. et al. 2010, "Effect of a post-deposition anneal on Al_2O_3/Si interface properties", Proc. 35th IEEE PVSC, Honolulu, Hawaii, USA, p. 891.

[17] Rothschild, A. et al. 2010, "ALD-Al_2O_3 passivation for solar cells: charge investigation", *Proc. 25th EU PVSEC*, Valencia, Spain, p. 1382.

[18] Simoen, E. et al. 2011, "Impact of Forming Gas Annealing and Firing on the Al_2O_3/p-Si Interface State Spectrum", *Electrochem. Solid-State Lett.*, Vol. 14, No. 9, pp. H362–H364.

[19] Rothschild, A. et al. 2011, "Al_2O_3 surface passivation: electrical characterization using the Quantox tool", *Proc. 37th IEEE PVSC*, Seattle, Washington, USA [in press].

[20] Richter, A. et al. 2010, "Firing stable Al_2O_3/SiN_x layer stack passivation for the front side boron emitter of n-type silicon solar cells", *Proc. 25th EU PVSEC*, Valencia, Spain, p. 1453.

[21] Schmidt, J. et al. 2010, "Surface passivation of silicon solar cells using industrially relevant Al_2O_3 deposition techniques", *PVI*, 10th edn, p. 52.

[22] Chunduri, S.K. 2011, "Looking back to go forth", *Photon Inter.*, March, p. 146.

About the Authors

Aude Rothschild received her Ph.D. degree in inorganic chemistry of materials from the University of Versailles St Quentin, France, in 1997. From 1998 to 1999, she carried out work on inorganic nanotubes at the Weizmann Institute of Science in Israel. Aude has been with imec since 2000 and has worked on medium-k and high-k dielectrics for CMOS and NVM applications. Her current research area is dielectric passivation of solar cells with Al_2O_3.

Bart Vermang is a Ph.D. student at the University of Leuven, Belgium, while performing his research within imec. In 2005 he graduated in physics from the University of Ghent, Belgium, having carried out research for his master's thesis in surface science studies of model metallic catalyst systems at the Norwegian University of Science and Technology. Bart's present research focuses on the integration of Al_2O_3 in surface passivation of industrial Si solar cells.

Hans Goverde is a master's student at the Eindhoven University of Technology. Hans is currently doing research at imec on the integration of Al_2O_3 in surface passivation of industrial Si solar cells.

Enquiries

Aude Rothschild
imec
Kapeldreef 75
3001 Leuven
Belgium
Tel: +32 16 28 83 47
Fax: +32 16 28 10 97
Email : Aude.Rothschild@imec.be
Web: www.imec.be